

实际环境下单脉冲位置调制量子增强接收机分析

张卫川, 潘青, 苏力华, 吴田宜, 东晨*

国防科技大学信息通信学院, 湖北 武汉 430030

摘要 脉冲位置调制具有高能效比的特点,对于抵抗自由空间信道干扰具有良好效果,而基于脉冲编码调制的联合检测量子增强接收机能够突破标准量子极限,进一步降低其误码率并逼近 Helstrom 极限。研究了影响单脉冲位置调制联合检测量子增强接收机的实际因素,分析了干涉度、暗计数和探测效率对单脉冲位置调制联合检测量子增强接收机误码率的影响,为实际量子增强接收机的参数选择提供了理论参考。仿真结果表明:随着平均光子数的增加,非理想的干涉度会使误码率先减后增,其极小值点大小与干涉度呈正相关;暗计数的存在会使误码率最终收敛于一个定值,该定值是暗计数的单调减函数;非理想的探测效率使得误码率呈指数级递减,且递减速率随探测效率的提升而增大。

关键词 量子光学; 单脉冲位置调制; 联合检测; 量子增强接收机; 干涉度; 暗计数; 探测效率

中图分类号 TN929.1

文献标志码 A

DOI: 10.3788/CJL220941

1 引言

开关键控(OOK)已经成为自由空间光通信中应用广泛的调制方式之一。脉冲位置调制(PPM)作为由 OOK 经编码后得到的一种调制方式,具有高能效比的特点,其通过降低占空比,能够获得更高的峰值光功率^[1],可克服大气湍流和暗计数^[2]等因素对信号的不良影响,获得更高的信噪比,具有较好的信道抗干扰能力,在大气乃至深空光通信^[3]等领域中具有重要的应用价值。

在脉冲位置调制通信系统中,经典接收机通常以直接检测作为脉冲位置调制信号的检测方式,其误码性能受限于标准量子极限(SQL)^[4]。但在量子理论下,其对应的通信系统能够获得比经典通信系统更多的信息^[5-6]。1976年,Helstrom^[7]提出了量子检测与估计理论,根据测量的准确度得出了量子理论中区分物理态的最小误码极限(Helstrom 极限),较 SQL 有指数倍的增益。1982年,Dolinar^[8-9]提出了条件归零量子接收机的理论模型,通过实时调整归零策略实现了时隙间的联合检测,克服了散粒噪声带来的影响。在理想情况下,该接收机在理论上能够突破 SQL,但是在光子数较大时与 Helstrom 极限有 3 dB 的差距。2012年,Chen 等^[10]首次实现了 4-PPM 信号条件归零接收机的实验验证^[10]。2016 年以来,陈田等^[11-13]针对脉冲位置调制信号设计了

基于最优控制理论的联合检测量子增强接收机,该接收机具有与条件脉冲归零量子接收机相同的性能。

然而,目前关于实际因素对脉冲位置调制量子增强接收机误码性能影响的研究鲜有报道。本文基于 4-PPM 信号调制,分析了干涉度、暗计数和探测效率等主要实际因素对单脉冲位置调制联合检测量子增强接收机误码性能的影响,为后续开展量子增强接收机设计与实验提供了理论参考。

2 基本原理

量子增强接收机通过位移算符作用于编码相干态,将经典测量转化为光子数的测量,因此接收机的误码性能突破 SQL 并逼近 Helstrom 极限。量子增强接收机采用正定算符取值测度(POVM),可以利用经典接收机所不能利用的量子信息,提升通信系统在误码率等方面的性能^[14-15]。同时,基于脉冲位置调制的量子增强接收机能够进一步提高通信系统性能。

单脉冲编码调制通过改变脉冲在码字中不同时隙中的位置,实现对信息的调制和传输,其联合检测量子增强接收机的系统模型如图 1 所示。

以 4-PPM 信号为例,其合法码字有 0001、0010、0100、1000。如图 1 所示,若码字为 0010,则在四个时隙中依次输入 $|0\rangle, |\alpha\rangle, |0\rangle, |0\rangle$ 四次光信号,其他码字

收稿日期: 2022-06-06; 修回日期: 2022-07-10; 录用日期: 2022-08-18; 网络首发日期: 2022-08-28

基金项目: 国家自然科学基金(62101559)、国防科技 173 计划技术领域基金(2021-JCJQ-JJ-0510)、国防科技大学校内科研项目(ZK22-09)

通信作者: *dongchengfkd@163.com

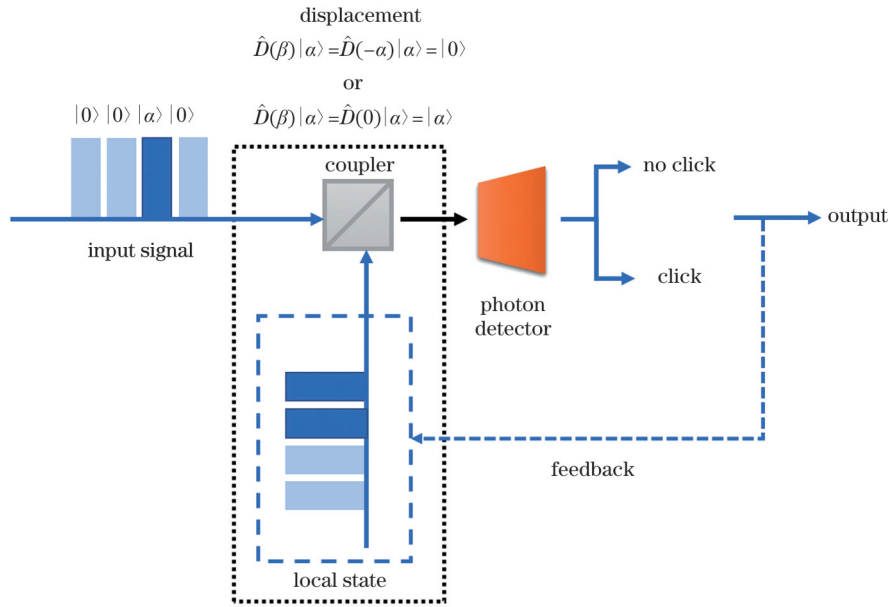


图 1 基于脉冲位置调制信号的联合检测量子增强接收机系统结构

Fig. 1 System structure of joint detection quantum enhanced receiver based on pulse position modulation signal

同理。这四个码字的先验概率相同,均为 1/4。

承载码字信息的信号光由信道逐时隙地传入接收机,首先在耦合器中与本振光作用(位移操作);接着进入单光子探测器,对位移后的光信号进行直接检测;然后探测器将检测结果实时反馈给本振光,根据已有策略确定对下一时隙作用的位移算子;重复上述操作,直至该码字的所有时隙检测完毕,最终输出判决结果。

在单脉冲位置调制联合检测量子接收机中,脉冲的检测方式有两种,即归零(位移)后直接检测和直接检测。在实际环境下,在耦合器中,当对第 m 个时隙的信号光 $|\alpha_m\rangle$ 和本振光 $|\beta_m\rangle$ 进行位移操作后,其光强 $(I_m)^{[15-16]}$ 可以表示为

$$I_m = (1 - \xi)(|\alpha_m|^2 + |\beta_m|^2) + \xi|\alpha_m + \beta_m|^2, \quad (1)$$

式中: $m = 1, 2, \dots, M$, 其中 M 为脉冲位置调制中合法码字的比特数; α_m 为信号光的幅值; β_m 为本振光的幅值; ξ 为干涉度。

在归零(位移)后直接检测中, $|\beta_m\rangle = -|\alpha\rangle$ 。若 $|\alpha_m\rangle = |\alpha\rangle$, 则该时隙上有脉冲信号, 对其进行单光子检测, 没有检测到光子(即正确接收)的概率为

$$P_m = \exp(-\nu - \eta I_m) = \exp[-\nu - 2\eta(1 - \xi)\bar{n}], \quad (2)$$

式中: $\bar{n} = |\alpha|^2$ 为平均光子数; η 和 ν 分别为单光子探测器的探测效率和暗计数。

若 $|\alpha_m\rangle = |0\rangle$, 即该时隙上无脉冲, 则检测到光子(即正确接收)的概率为

$$P_m = 1 - \exp(-\nu - \eta I_m) = 1 - \exp[-\nu - 2\eta(1 - \xi)\bar{n}]. \quad (3)$$

在直接检测中, 由于没有位移操作, 即 $|\beta_m\rangle = |0\rangle$, 耦合器的输出只有信号光。若 $|\alpha_m\rangle = |\alpha\rangle$, 则检测到光子(即正确接收)的概率的计算式同式(3)。

若 $|\alpha_m\rangle = |0\rangle$, 则在单光子检测时, 未检测到光子(即正确接收)的概率为

$$P_m = \exp(-\nu). \quad (4)$$

针对 4-PPM 信号的联合检测量子增强接收机的反馈控制策略如图 2 所示。

根据上述决策树, 可以逐时隙地代入实际因素的参数。经计算得到联合检测量子增强接收机的误码性能为

$$P_{e4PPM}^{CPN} = 1 - \frac{1}{4}(P_{suc1} + P_{suc2} + P_{suc3} + P_{suc4}), \quad (5)$$

式中: P_{suc1} 、 P_{suc2} 、 P_{suc3} 、 P_{suc4} 分别对应码字 0001、0010、0100、1000 正确判决的概率。由决策树可知

$$\begin{cases} P_{suc1} = P_{0001|0001} \\ P_{suc2} = P_{0010|0011} + P_{0010|0010} \\ P_{suc3} = P_{0100|0101} + P_{0100|0110} + P_{0100|0100} \\ P_{suc4} = P_{1000|1001} + P_{1000|1010} + P_{1000|1100} + P_{1000|1000} \end{cases} \quad (6)$$

以 $P_{0010|0011}$ 为例, 其表示发送码字为 0010 且检测结果为 0011 时判决结果仍为 0010 的概率, 其他参数同理。关于 $P_{0010|0011}$ 的具体推导, 可由决策树逐时隙地进行计算。

第 1 个时隙归零后直接检测时, 未检测到光子的概率为

$$P_1 = \exp(-\nu - \eta\bar{n}). \quad (7)$$

第 2 个时隙直接检测时, 检测到光子的概率为

$$P_2 = 1 - \exp(-\nu - \eta\bar{n}). \quad (8)$$

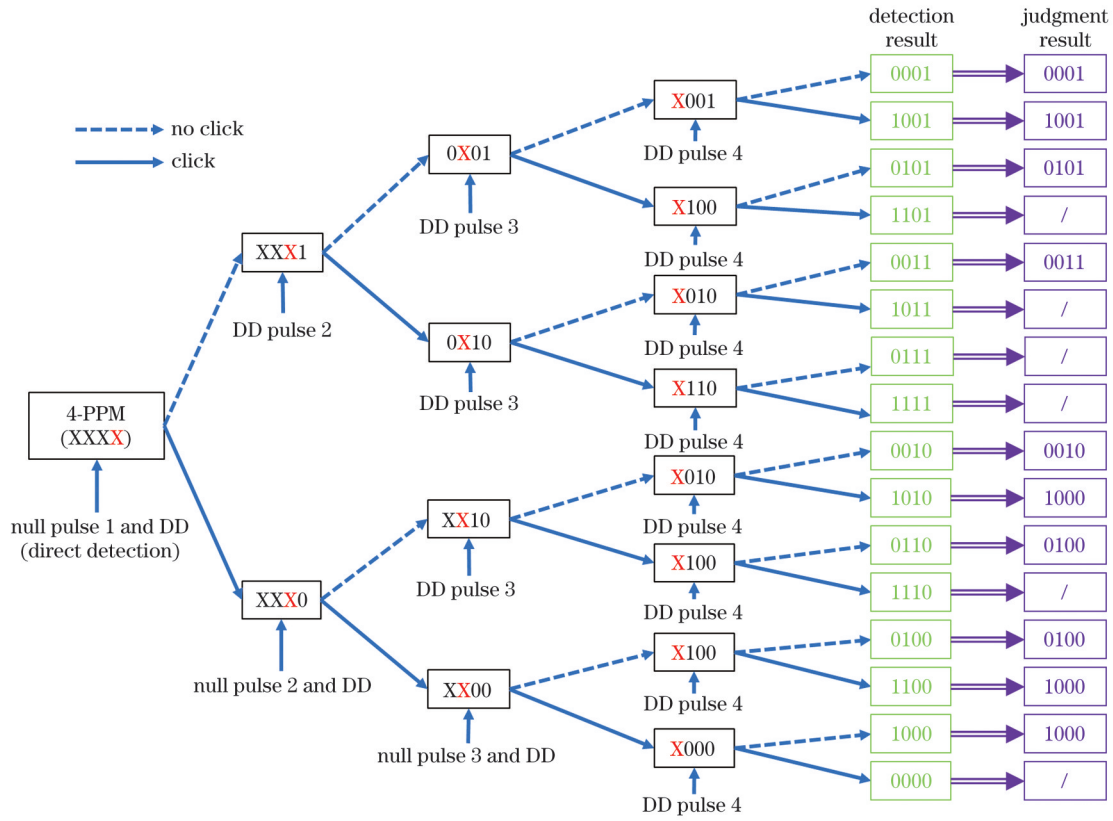


图 2 考虑实际因素时联合检测量子增强接收机决策树示意图

Fig. 2 Schematic of decision tree of joint detection quantum enhanced receiver considering practical factors

第 3 个时隙直接检测时, 未检测到光子的概率为

$$P_3 = \exp(-\nu). \quad (9)$$

计算式同式(9)。则

$$P_{0001|0001} = P_1 P_2 P_3 P_4. \quad (10)$$

第 4 个时隙直接检测时, 未检测到光子的概率的

其他参数的推导同理, 最终可以得到结果为

$$\begin{cases}
 P_{0001|0001} = \exp[-4\nu - 2\eta(1 - \xi)\bar{n}] \\
 P_{0010|0011} = [1 - \exp(-\nu - \eta\bar{n})] \exp(-3\nu - \eta\bar{n}) \\
 P_{0010|0010} = [1 - \exp(-\nu - \eta\bar{n})] \exp[-3\nu - 2\eta(1 - \xi)\bar{n}] \\
 P_{0100|0101} = [1 - \exp(-\nu - \eta\bar{n})] \exp(-3\nu - \eta\bar{n}) \\
 P_{0100|0110} = [1 - \exp(-\nu - \eta\bar{n})]^2 \exp(-2\nu - \eta\bar{n}) \\
 P_{0100|0100} = [1 - \exp(-\nu - \eta\bar{n})]^2 \exp[-2\nu - 2\eta(1 - \xi)\bar{n}] \\
 P_{1000|1001} = [1 - \exp(-\nu - \eta\bar{n})] \exp(-3\nu - \eta\bar{n}) \\
 P_{1000|1010} = [1 - \exp(-\nu - \eta\bar{n})]^2 \exp(-2\nu - \eta\bar{n}) \\
 P_{1000|1100} = [1 - \exp(-\nu - \eta\bar{n})]^3 \exp(-\nu - \eta\bar{n}) \\
 P_{1000|1000} = [1 - \exp(-\nu - \eta\bar{n})]^3 \exp[-\nu - 2\eta(1 - \xi)\bar{n}]
 \end{cases} \quad (11)$$

3 仿真分析

本节对上述模型进行蒙特卡罗仿真, 分析了联合检测量子增强接收机中干涉度、暗计数以及探测效率

对系统性能的影响, 同时对该影响、SQL、Helstrom 极限和接收机的理想性能进行了比较, 具体参数如表 1 所示。

当暗计数和探测效率取理想值($\nu=0, \eta=100\%$)

表 1 主要仿真参数设置

Table 1 Main simulation parameter settings

Influence factor	Setting value
Interference visibility	90.00%, 94.00%, 98.00%, 99.00%, 99.50%, 99.90%, 99.99%
Dark count	10^{-2} , 5×10^{-2} , 10^{-3} , 5×10^{-3} , 10^{-4} , 5×10^{-4} , 10^{-5}
Detection efficiency	60%, 65%, 70%, 75%, 80%, 85%, 90%, 95%

时,不同干涉度下联合检测量子增强接收机的误码性能如图 3 所示,其中,T 表示误码率理论值,S 表示误码率仿真值,CPN 表示条件脉冲归零。在干涉度一定时,随着平均光子数的增加,其误码率先减后增。且提高干涉度时,误码率的极小值减小,对应的极小值点(平均光子数)大小增大。其原因是:在干涉度不变的情况下,随着光子基数的变大,在相同的时间内,会有更多的脉冲信号无法归零。当干涉度为 90.00% 时,若平均光子数小于 1.10,接收机的误码率与 SQL 相比几乎没有优势,前者的极小值甚至劣于同一平均光子数下的 SQL。而当干涉度提升至 99.90% 时,误码率在平均光子数约为 3.60 处取得极小值,在平均光子数大于 4.40 时劣于 SQL,且在平均光子数较小时,能够逼近理想性能,与 Helstrom 极限相差约 3 dB。

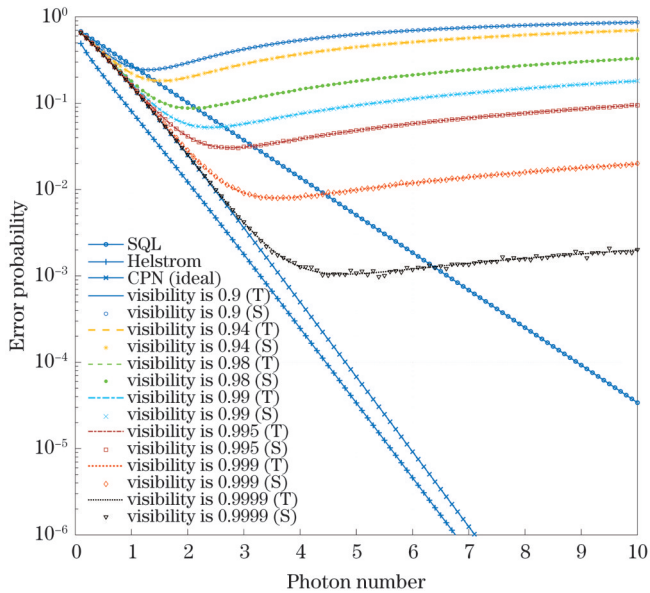


图 3 不同干涉度下 4-PPM 联合检测量子增强接收机的误码性能

Fig. 3 Bit error performance of 4-PPM joint detection quantum enhanced receiver with different interference visibility

当干涉度和探测效率取理想值($\xi=100\%$, $\eta=100\%$)时,不同暗计数下联合检测量子增强接收机的误码性能如图 4 所示。当不改变暗计数时,随着平均光子数的增加,误码率逐渐收敛于某个极限;且暗计数越小,该极限也越小,该极限优于 SQL 时

所对应的平均光子数范围也越大。经计算得该极限为

$$\lim_{\substack{n \rightarrow \infty \\ \xi, \eta = 0}} P_{e4PPM}^{CPN} = 1 - \frac{1}{4} [\exp(-\nu) + \exp(-2\nu) + \exp(-3\nu) + \exp(-4\nu)] \quad (12)$$

当暗计数为 10^{-2} 时,接收机的误码率极限约为 2.46×10^{-2} ,在平均光子数小于 3.30 时其误码性能均优于 SQL;而当暗计数下降至 5.00×10^{-5} 时,该极限也下降至 1.25×10^{-4} ,接收机误码率优于 SQL 时所对应的最大平均光子数也提升至 8.70 左右,且当平均光子数较小时,误码率也逼近 Helstrom 极限。

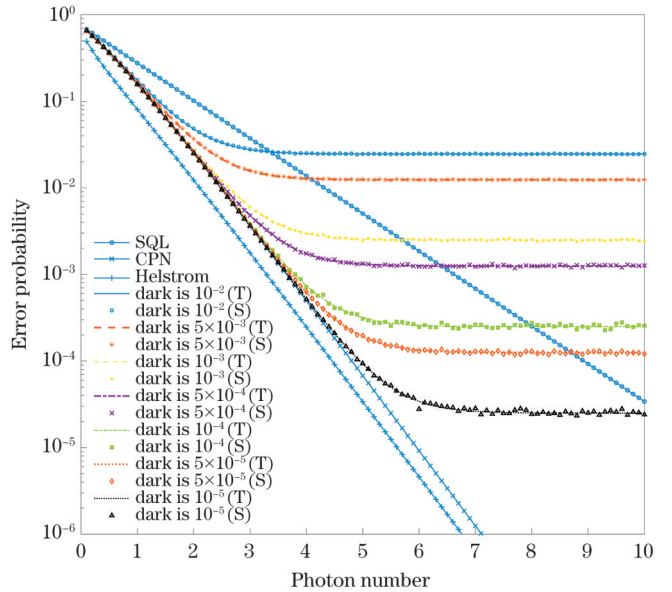


图 4 不同暗计数下 4-PPM 联合检测量子增强接收机的误码性能

Fig. 4 Bit error performance of 4-PPM joint detection quantum enhanced receiver under different dark counts

当干涉度和暗计数取理想值($\xi=100\%$, $\nu=0$)时,不同探测效率下联合检测量子增强接收机的误码性能如图 5 所示。当探测效率恒定时,随着平均光子数的增加,其误码率呈指数级减小;当探测效率低至 0.6 时,接收机的误码率仍优于 SQL;且探测效率越大,误码率减小的速率越大,与接收机的理想性能和 Helstrom 极限也更接近;当探测效率达到 0.95、平均光子数为 6.50 时,误码率约为 6.48×10^{-6} ,与 Helstrom 极限相差约 5.8 dB。

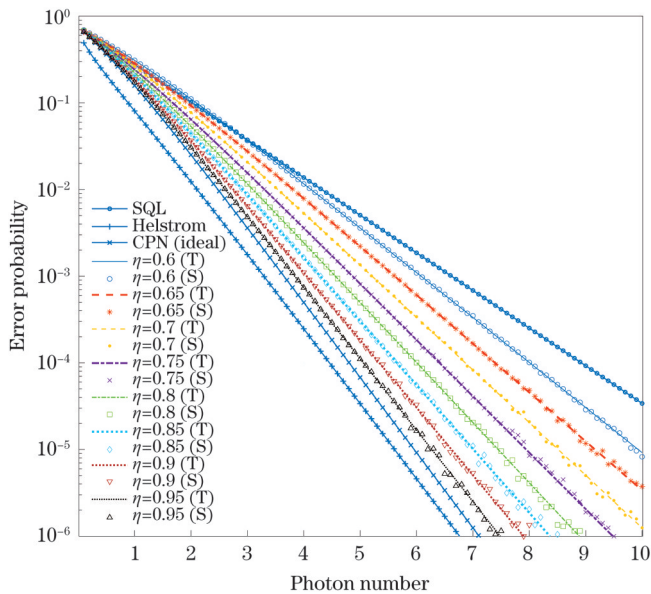


图5 不同探测效率下4-PPM联合检测量子增强接收机的误码性能

Fig. 5 Bit error performance of 4-PPM joint detector quantum enhanced receiver with different detection efficiencies

4 结 论

研究了实际条件下单脉冲位置调制联合检测量子增强接收机的误码性能与各种因素的关系,分析了干涉度、暗计数和探测效率对接收机误码率的影响。仿真结果表明:随着平均光子数的增加,非理想的干涉度使得误码率先减后增,极小值点大小与干涉度呈正相关;暗计数的存在使得误码率收敛于某一极限,该极限是暗计数的单调减函数;非理想的探测效率会使误码率呈指数级递减,且探测效率越高,误码率递减速率越大。在实验中,通过选取数量适中的输入光的平均光子数并在搭建接收机时调节本振光的强度和偏振来提升干涉度,通过选用具有更高探测效率和更低暗计数的单光子探测器,在节约能量的前提下,提升实际条件下单脉冲位置调制联合检测量子增强接收机的误码性能。

未来将该研究推广至多脉冲位置调制,进一步讨论实际因素对更高码率的脉冲位置调制的影响,并制定合适的反馈策略,减少条件脉冲归零策略中的不确定因素,进而减小码字判决的错误概率。

参 考 文 献

[1] Caplan D O, Stevens M L, Boroson D M, et al. High-sensitivity

variable-rate transmit/receive architecture[C]//IEEE Lasers and Electro-Optics Society 1999 Annual Meeting, November 8-11, 1999, San Francisco, CA, USA. New York: IEEE Press, 1999: 297-298.

[2] 刘旭超, 李华贵, 孙时伦, 等. 湍流信道下光量子通信系统误码分析及优化[J]. 光学学报, 2022, 42(3): 0327018.
Liu X C, Li H G, Sun S L, et al. Bit error analysis and optimization of optical quantum communication system under turbulent channel[J]. Acta Optica Sinica, 2022, 42(3): 0327018.

[3] Sun X L, Skillman D R, Hoffman E D, et al. Free space laser communication experiments from Earth to the Lunar Reconnaissance Orbiter in lunar orbit[J]. Optics Express, 2013, 21(2): 1865-1871.

[4] Wozencraft J M, Jacobs I M. Principles of communication engineering[M]. New York: Wiley, 1965

[5] 刘翔钊, 左小杰, 闫智辉, 等. 基于光学参量放大器的量子干涉仪的分析[J]. 光学学报, 2022, 42(3): 0327013.
Liu Y Z, Zuo X J, Yan Z H, et al. Analysis of quantum interferometer based on optical parametric amplifier[J]. Acta Optica Sinica, 2022, 42(3): 0327013.

[6] 袁媛, 钮月萍, 龚尚庆, 等. 集体测量估计量子相干性的性能研究[J]. 光学学报, 2022, 42(3): 0327014.
Yuan Y, Niu Y P, Gong S Q, et al. Performance of collective measurement to estimate quantum coherence[J]. Acta Optica Sinica, 2022, 42(3): 0327014.

[7] Helstrom C W. Quantum detection and estimation theory[M]. New York: Academic Press, 1976.

[8] Dolinar S J. A class of optical receivers using optical feedback[D]. Massachusetts: Massachusetts Institute of Technology, 1976.

[9] Dolinar S J. A near-optimum receiver structure for the detection of M-ary optical PPM signals[EB/OL]. (1983-02-15) [2022-02-04]. <https://ntrs.nasa.gov/citations/19830011498>.

[10] Chen J, Habif J L, Dutton Z, et al. Optical codeword demodulation with error rates below the standard quantum limit using a conditional nulling receiver[J]. Nature Photonics, 2012, 6(6): 374-379.

[11] 陈田. 空间光通信系统中量子接收机的设计与实验研究[D]. 合肥: 中国科学技术大学, 2018.
Chen T. Design and experimental study of quantum receivers in space optical communication system[D]. Hefei: University of Science and Technology of China, 2018.

[12] 左元. 光通信中量子接收机的理论与初步实验研究[D]. 合肥: 中国科学技术大学, 2016.
Zuo Y. Theory analysis and preliminary experimental study of quantum receivers in optical communication system[D]. Hefei: University of Science and Technology of China, 2016.

[13] 董菲. 激光通信系统自适应测量量子接收机研究[D]. 合肥: 中国科学技术大学, 2019.
Dong F. Study of adaptive measurement quantum receivers in laser communication system[D]. Hefei: University of Science and Technology of China, 2019.

[14] Gisin N, Thew R. Quantum communication[J]. Nature Photonics, 2007, 1(3): 165-171.

[15] Cariolaro G. Quantum Communications[M]. Cham: Springer, 2015.

[16] Izumi S, Neergaard-Nielsen J S, Miki S, et al. Experimental demonstration of a quantum receiver beating the standard quantum limit at telecom wavelength[J]. Physical Review Applied, 2020, 13(5): 054015.

Analysis of Single-Pulse Position Modulation Quantum Enhanced Receiver in Practical Environments

Zhang Weichuan, Pan Qing, Su Lihua, Wu Tianyi, Dong Chen*

Institute of Information and Communication, National University of Defense Technology, Wuhan 430030, Hubei, China

Abstract

Objective Pulse position modulation, which is a modulation method obtained from the on-off keying (OOK) after encoding, has the characteristic of a high energy efficiency ratio, which increases peak optical power by reducing the duty cycle to overcome the adverse effects of factors such as atmospheric turbulence and dark counts on the signal. It also increases the signal-to-noise ratio, giving it better channel interference immunity, which is important in a wide range of applications in atmospheric and even deep-space optical communications. In pulse position modulation communication systems, classical receivers usually use direct detection to detect pulse position modulated signals, and their bit error rate (BER) performance is limited to the standard quantum limit (SQL). However, in quantum theory, their counterparts, which can obtain more information than classical communication systems, increase the BER performance to the Helstrom limit. However, there is a lack of relevant studies on the effects of practical factors on the BER performance of pulse position modulated quantum-enhanced receivers. In this study, we analyze the effects of the main practical factors, interference visibility, dark counts, and detection efficiency on the BER performance of a single pulse position modulated joint detection quantum-enhanced receivers based on 4-PPM (PPM, pulse position modulation) signal modulation. We also provide a theoretical reference for the subsequent development of quantum-enhanced receiver design and experiments.

Methods First, the structure of the joint detection quantum-enhanced receiver system for pulse position modulated signals is introduced. Second, a decision-tree model of the corresponding feedback control strategy is established, from which the theoretical BER performance of the joint detection quantum-enhanced receiver is obtained. Then, the effects of practical factors such as interference visibility, dark counts, and detection efficiency on the system performance are analyzed by Monte Carlo simulation and compared with SQL, the Helstrom limit, and the ideal performance of the receiver to determine the influence mechanisms of various practical factors.

Results and Discussions The simulation results show that as the average number of photons increases, the non-ideal interference visibility causes the bit error to first decrease and then increase, and its minimum point value is positively correlated with the interference visibility (Fig. 3). The existence of dark counts causes the bit error rate to converge to a fixed value, which is a monotonically decreasing function of dark counts (Fig. 4). Moreover, the non-ideal detection efficiency causes the bit error rate to decrease exponentially and the deceleration rate to increase with the detection efficiency (Fig. 5).

Conclusions In the experiment, by adjusting the moderate numbers of average photons of input signals and the intensity and polarization of the local oscillator to obtain high interference visibility, and applying the single photon detector with high detection efficiency and low dark count, the BER performance of the single-pulse position modulation quantum-enhanced receiver can be improved under practical conditions while saving energy. In future, this approach could also be extended to multipulse position modulation to further determine the effects of practical factors on pulse position modulation at higher code rates. Meanwhile, the development of a suitable feedback strategy to reduce uncertainties in the conditional pulse nulling strategy could reduce the probability of code-word judgment errors.

Key words quantum optics; single-pulse position modulation; joint detection; quantum-enhanced receiver; interference visibility; dark count; detection efficiency